

**Dielectric Properties of High Coercivity Barium Ferrite-Natural Rubber Composites**

Journal:	<i>Journal of Applied Polymer Science</i>
Manuscript ID:	APP-2009-11-3595.R1
Wiley - Manuscript type:	Research Article
Keywords:	dielectric properties, composites, conducting polymers



## Dielectric Properties of High Coercivity Barium Ferrite-Natural Rubber Composites

**Mamoud H. Makled**

Faculty of Science, Physics Department, Benha University, 13518 Benha , Egypt.

---

### Abstract

The effect of frequency, temperature and  $\text{BaFe}_{12}\text{O}_{19}$  (BF) content on the dielectric constant  $\epsilon'$ , dielectric loss  $\epsilon''$  and  $\tan\delta$  were studied for barium ferrite - natural rubber composites (RFC). The dielectric constant for barium ferrite was related to the preparation method meanwhile the dielectric constant of natural rubber (NR) is relatively large compared to the theoretical value. The results showed  $\epsilon'$ ,  $\epsilon''$  and  $\tan\delta$  for RFC decrease as the frequency increases however at higher frequencies the effect significantly weakens. At low ferrite loading the dielectric properties are strongly influenced by BF content. Strong correlation between magnetic initial permeability and dielectric constant for hard magnetic material polymer composites was also observed. Increasing the content of barium ferrite in NR matrix enhances both  $\epsilon''$  and  $\tan\delta$ .

*Key Words: polymer composites; dielectric properties ; hard ferrite ; rubber*

---

Corresponding author: [mahmoud.makld@fsc.bu.edu.eg](mailto:mahmoud.makld@fsc.bu.edu.eg)

## INTRODUCTION

Recently, there is a growing demand for multifunctional composites to meet the further requirements of electronic components. By incorporation of ferrites into an elastomer matrix, one can modify the dielectric behaviors and impart magnetic properties to the composites. Hex-ferrites are a major class among the ferrite materials due to their applications as permanent magnets and high-density magnetic recording media. Another advantage is the chemical stability of these oxides which makes them environmentally safe<sup>1</sup>.

The effective permittivity and conductivity of a composite is a complicated function of the physical properties of the individual components, such as, shape and particle size distribution, porosity, volume loading, the interaction between filler and insulating matrix, sulfur content or the degree of cross linked, etc<sup>2-9</sup>.

In the literature, most of the data refers to systems composed of soft ferrite polymer composites and mention little about barium ferrite or barium ferrite polymer composites<sup>10-15</sup>. With this in mind, dielectric properties of barium ferrite (BF) powder varies querulously from about 3 to 40 at 1 MHz depending on the preparation methods, particle size and coercivity<sup>16-20</sup>.

Ultimately, due to the unlimited number of parameters one can utilize to control the physical properties of the composite, the change in the composite's properties with compositional variations cannot usually be described using a simple formalism or one model. Thus, the fundamental study and measurement of the properties of composite media remains an active area of basic and applied research<sup>21-26</sup>.

Natural rubber (NR) is selected as a matrix for mixing the present ferrite as it is commercially available and low in cost and the dielectric properties are less effected by frequency and temperature.

This work forms part of a comprehensive study focusing on the fabrication of hard magnetic ferrite and rubber-ferrite composites (RFC), and study their physical properties (Curing, mechanical, magnetic, and electrical properties) as a function of ferrite content. The present manuscript is an attempt to understand the dielectric behaviors in the case of high coercivity materials –polymer composites as a function of ferrite loading, frequency and temperature.

## EXPERIMENTAL

### Materials

Hexagonal barium ferrite  $\text{BaFe}_{12}\text{O}_{19}$  (BF) phase with variable coercivity, saturation magnetization and particle size were prepared by a coprecipitation method according to Makled et.al.<sup>27</sup>. BF with 5.2 KOe coercivity, 67 emu/g saturation magnetization and 45-200  $\mu\text{m}$  particle size was selected. After pre-characterization BF was mixed with a natural rubber ADS (air dried sheet) by using various loadings up to 120 Phr (Part per hundred rubber) to form rubber-ferrite composites (RFC). The composites were prepared in a two-roll mixing mill and after homogenization were cured and molded into thin sheets of 1–2 mm in thickness at 150 °C using a hydraulic press according to ASTM D-15. The recipe used for this study, Cure characteristics, magnetic and mechanical properties and the change of RFC density with BF loading were reported elsewhere<sup>28-29</sup>.

### Techniques

Ferrite samples were prepared by compressing the powder into a disk at room temperature with 1cm diameter and 1.5 mm thick (under static pressure  $3 \times 10^3 \text{ Kg cm}^{-2}$ ) for all dielectric studies. The RFC samples were cut from vulcanized sheets with a 1 mm thickness. The capacitance, resistance and dissipation factors were measured directly by using [ Hioki 3532 LCR High tester, Japan ] from 100KHz to 5MHz. Silver paint was used to coat either side of the samples and copper wires were then fixed to each sides to form electrodes. Pre-calibration for the LCR tester and the shield connected cables were performed prior to measurements acquisition. Temperature based studies were carried out using a non inductive furnace up to 120 °C at a heating rate of 5 °C// min. A Micromeritics (TriStar 3000) was employed for porosity measurements. Scanning electron micrographs (SEM) for RFC were obtained from a fractured and polished surface under liquid nitrogen. The resulting surface was coated with carbon prior to the SEM investigation.

## RESULTS AND DISCUSSION

Figure 1 shows the microstructures of RFC for (a) 30 and (b) 120 Phr respectively.

The variation of particle sizes, the broad particle distribution, and the homogeneous dispersion were noticed. Also there is no tendency of agglomerates formation or percolation in the present RFC at maximum BF loading.

The dielectric constant  $\epsilon'$  and loss tangent  $\tan\delta$  of BF versus frequency at different temperatures are shown in Figure 2. At lower frequencies  $\epsilon'$  decreases rapidly with increasing frequency. While at higher frequencies, the decrease in  $\epsilon'$  becomes less pronounced. This is the normal dielectric behavior of ferrite which could be explained by Koops theory and obey Maxwell Wagner model for interfacial polarization<sup>30</sup>. Even the polar materials possess a very high dielectric constant<sup>31</sup>. Based on these features the dielectric constant for the present ferrite is relatively low. As shown in Figure 2(a),  $\epsilon'$  is 25 at 1 MHz and room temperature, and increases to 43 at 423 K recording 10 and 17 K at 5 MHz respectively. These values appear to be completely dependent on the preparation of BF. As an example, the present ferrite has a measured porosity = 17 and the particles have a porous surface<sup>29</sup>. These physical properties weaken the dielectric constant<sup>17</sup>. Contrary to this, the particle size is large 45-200  $\mu\text{m}$ , which enhances the dielectric constant due to the increase in interfacial area between conducting ferrite grains separated by the second poorly conducting thin layer of grain boundaries, leading to the increase in material capacitance. In previous work, BF was prepared by ceramic powdered methods with particle size  $> 200 \mu\text{m}$ , low porosity and 1.5 KOe coercivity. These characteristics emerged  $\epsilon' = 500$  at 100 KHz<sup>32</sup>. While  $\epsilon' = 40$  for the present ferrite at the same frequency. The acquired result suggests, strong interaction between the strong magnetic domains of BF. On the other hand the dielectric constant of the powder is always obtained by measuring compacted samples, therefore it is obvious that there exists larger stress interaction between nanoparticles in this kind of samples, where the measured values cannot reveal the intrinsic dielectric properties. However in composite polymer system, when the concentration of inorganic nanoparticles is small, interactions between nanoparticles can be ignored<sup>33</sup>.

Increasing the temperature thermally activates the electron hopping between  $\text{Fe}^{2+}$  and  $\text{Fe}^{3+}$ . This electron hopping causes local displacement in the direction of the applied electric field, which induces dielectric polarization in ferrite<sup>34</sup>. As a result, the dielectric polarization increases causing an increase in dielectric constant and  $\tan \delta$ .

Figure 3 represents the variation of  $\epsilon'$  and  $\tan\delta$  as a function of frequency for NR at different temperatures. Both  $\epsilon'$  and  $\tan\delta$  for NR are less dependent on frequency and temperature than BF due to the absence of polarization and ionic properties of the material. In general, the temperature and frequency dependence of  $\epsilon'$  is controlled by the polarity of the polymer. For a non-polar material,  $\epsilon'$  equals the square of the refractive index. NR is a non-polar molecule, which has a refractive index of 1.59, and hence  $\epsilon' = 2.54$ <sup>35</sup>. The recorded experimental values are higher than the theoretical one, this may have occurred due to the presence of interfacial polarization, which arises due to the presence of impurities such as the compounding ingredients. The values of  $\epsilon'$  for NR at high frequencies are about 2.5 for all temperature ranges, which can be ascribed to the mobility of a polar group in the polymer chains which is too slow to contribute to the dielectric constant at high frequencies<sup>36</sup>.

The variation of the dielectric constant with BF loading at different frequencies is represented in Figure 4. The effects of the dielectric constant due to frequency changes are moderate between rubber and ferrite. These observations can be explained according to the conduction in composites, which is controlled by an electron emission process between adjacent conducting particles, across the thin film of the polymer layer separates them<sup>37</sup>. All samples recorded a sharp increase in  $\epsilon'$  with increasing BF content up to 30 Phr ferrite loading. At high ferrite loading the dependence of  $\epsilon'$  on ferrite content becomes minimal. Similar behaviors were recorded for Strontium ferrite–NR composites by M.A. Solomon et al.<sup>15</sup>. These results disagree with those reported for any filler and soft ferrite, even for low coercivity barium ferrite. Normally  $\epsilon'$  slightly increases when the filler content is increased at low filler loading. While after critical filler loading the dielectric constant becomes strongly dependent on filler content<sup>10,12,21,24,38,39</sup>. Results presented in Figure 4 demonstrate, the interaction between ferrite particles starts at 30 Phr considering the relative distances between ferrite particles are large as seen in Figure 1(a). This observation provides a strong case to suggest a strong interaction between the present ferrite particles is occurring.

To understand the behavior of the dielectric constant for hard magnetic material – polymer composites with filler loading. The initial magnetic permeability  $\mu$ , which is a function of domain wall motion, was calculated directly from the hysteresis loops at different BF loading<sup>28</sup> and is summarized in Figure 5. At low ferrite loading  $\mu$

significantly increases by increasing BF content, however at high ferrite loading  $\mu$  is less dependent on ferrite content. This behavior is very similar to the dependence of  $\epsilon'$  on BF content Figure 4. As the ferrite particles come closer to each other at certain volume fraction. Thus the interactions between the magnetic filler particles becomes stronger. In this composition, the magnetic domains are not affected by the applied field, which leads to less dependence of the magnetic and dielectric properties on BF content at high loading. It is also expected that, due to the strong magnetic interaction between ferrite particles which increase by increasing filler loading. This unsaturated and high polarity medium will act as a scattering center for the ions and hence introduce additional loss in ion exchange. This artificial Phenomena will lead to more affect to the dielectric properties specially at high loading of BF.

Based on this study, one can conclude that, the variation of dielectric constant for RFC with frequency and filler loading depends primarily on the ceramic filler even at very low concentration. However the effect of polymer is predominant in the case of temperature dependence due to the large separating distances between ferrite particles. From other point of view, the percolation phenomena is interestingly observed with the present RFC at 180 Phr is yet to be explained and is currently under investigation.

The variation of  $\tan \delta$  with ferrite content for BF-NR composites at room temperature are shown in Figure 6. The comparative data suggests that, increasing BF content in the NR matrix enhances both the  $\epsilon''$  and  $\tan \delta$ . At low ferrite content the values are close to those of NR, where by increasing BF loading RFC controls the dielectric properties.

## CONCLUSION

The dielectric constant and dielectric loss decrease when frequency is increased, which is the expected behavior of hexaferrites. Hard magnetic material- polymer composites are strongly affected by the interaction between magnetic particles, which directly governs their magnetic and electric properties. *The effect of NR is predominant with temperature variation of RFC*. All analyzed samples demonstrate a sharp increase in  $\epsilon'$  with increasing BF content up to 30 Phr ferrite loading, while at high ferrite loading the dependence of  $\epsilon'$  on ferrite content becomes minimal as a result of ferrite particles interaction.

### Figures Captions

- 1- **Figure 1** SEM images for the RFC , (a) 30 and (b) 120 Phr
- 2- **Figure 2** (a) Dielectric constant and (b)  $\tan \delta$  for BF as a function of frequency at different temperatures
- 3- **Figure 3** (a) Dielectric constant and (b)  $\tan \delta$  for NR as a function of frequency at different temperatures
- 4- **Figure 4** Dependence of the dielectric constant on BF loading for (a) 293 K , (b) 353 K and (c) 393 K
- 5- **Figure 5** The variation of magnetic initial permeability with BF loading for RFC
- 6- **Figure 6** Loss tangent as function of BF content at different frequencies

### References

- 1- Milke, E. C.; Rei, M.; De Souza, J. P.; Schaeffer, L. Int J Powder Metall 2001, 37, 47.
- 2- Han, Ki. C.; Choi, H. Do.; Moon, T. J.; Kim, W. S.; Kim, K. Y. J Mater Sci 1995, 30, 3567.
- 3- Psarras, G. C.; Manolakaki, E.; Tsangaris, G. M. Compos Part A 2003, 34, 1187.
- 4- Tuncer, E.; Gubanski, S. M. J Phys Condens Matter 2000, 12, 1873.
- 5- Yu, S.; Hing, P.; Hu, X. J Appl Phys 2000, 88, 398.
- 6- Chandra, A.; Srivastava, P. C.; Chandra, S. J Mater Sci 1995, 30, 3633.
- 7- Truong, V-T.; Codd, A R.; Forsyth, M. J Mater Sci 1994, 29, 4331.
- 8- Badawy, M. M. Polym Test 1996, 15, 507.
- 9- Punkka, E.; Laakso, J.; Stubb, H.; Kuivalainen, P. Phys Rev 1990, 41, 5914.
- 10- Soloman, M. A.; Kurian, P.; Anantharaman, M. R.; Joy, P. A. J Appl Polym Sci 2003, 89, 769.
- 11- Peko, M. Jean-Claude. Appl Phys Lett 1997, 71, 3730.
- 12- Yacubwicz, J.; Narkis, M.; Kenig, S. Polym Eng Sci 1990, 30, 469.
- 13- El-Mansy, M. K.; Shash, N. M.; Makled, M. H.; Diefallah, E. M. Mater Chem



- Phys 1998, 52, 71.
- 14- Saini, D. R.; Nadkarni, V. M.; Grover, P. D.; Nigam, K. D. P. *J Mater Sci* 1986, 21, 3710.
- 15- Soloman, M. A.; Kurian, P.; Anantharaman, M. R.; Joy, P. A. *J Elast Plast* 2005, 37, 109.
- 16- Dimri, M. C.; Kashyap, S. C.; Dube, D. C. *Ceram. Int* 2004, 30, 1623.
- 17- Yang, Q.; Zhang, H.; Liu, Y.; Wen, Q. *Mater Lett* 2009, 63, 406.
- 18- Wang, C.; Han, X.; Xu, P.; Wang, X.; Li, X.; Zhao, H. *J Alloys Compd* in press 2008, 09, 092.
- 19- Mallick, K. K.; Shepherd, P.; Green, R. J. *J Eur Ceram. Soc* 2007, 27, 2045.
- 20- Haijun, Z.; Zhichao, L.; Chenliang, M.; Xi, Y.; Liangying, Z.; Mingzhong, W. *Mater Chem Phys* 2003, 80, 129.
- 21- Fiske, T. J.; Gokturk, H. S.; Kalyon, D. M. *J Mater Sci* 1997, 32, 5551.
- 22- Sareni, B.; Krahenbuhl, L.; Beroual, A.; Brosseau, C. *J Appl Phys* 1996, 80, 1688.
- 23- Sareni, B.; Krahenbuhl, L.; Beroual, A. *J Appl Phys* 1996, 80, 4560.
- 24- Lux, F. *J Mater Sci* 1993, 28, 285.
- 25- Ruschau, G. R.; Yoshikawa, S.; Newnham, R. E. *J Appl Phys* 1992, 72, 953.
- 26- Mantese, J. V.; Micheli, A. L.; Dungan, D. F.; Geyer, R. G.; Baker-Jarvis, J.; Grosvenor, J. *J Appl Phys* 1996, 79, 1655.
- 27- Makled, H.; Matsui, T.; Tsuda, H.; Mabuchi, H.; El-Mansy, M. K.; Morii, K. *J Ceram Soc Jpn* 2004, 112, 200.
- 28- Makled, M. H.; Matsui, T.; Tsuda, H.; Mabuchi, H.; El-Mansy, M. K.; Morii, K. *J Mater Process Technol* 2005, 160, 229.
- 29- Makled, M. H.; Washiya, Y.; Tsuda, H.; Matsui, T. *J Appl Polym Sci*, 2009, 113, 3294.
- 30- Koops, C. G. *Phys Rev* 1951, 83, 121.
- 31- Bai, Y.; Cheng, Z.-Y.; Bharti, V.; Xu, H. S.; Zhang, Q. M. *Appl Phys Lett* 2000, 76, 3804.
- 32- Makled, M. H. M.Sc. study of the electrical conductivity behavior of metal oxide metal carbonate mixture. Faculty of Science, Benha University; 1996.
- 33- Shi, W.; Fang, C.; Guo, S.; Pan, Q.; Gu, Q.; Xu, D.; Ren, Q.; Wei, H.; Yu, J.

- Canad J Phys 2001, 79, 847.
- 34- El Hiti, M. A. J Magn Magn 1999, 192, 305.
- 35- Haseena A. P.; Unnikrishnan, G.; Kalaprasad, G. Compos Interfaces 2007, 14, 763.
- 36- Popielarz, R.; Chiang, C. K.; Nozaki, R.; Obrzut, J. Macromol 2001, 34, 5910.
- 37- Lalkishore, K.; RamKumar, K.; Satyam, M. J Appl Phys 1987, 61, 397.
- 38- Puryanti, D.; Ahmad, S. Hj.; Abdullah, M. Hj. Polym Plast Tech Eng 2006, 45, 561.
- 39- Doyle, T. W. J Appl Phys 1995, 78, 6165.

### Figures Captions

- 1- **Figure 1** SEM images for the RFC , (a) 30 and (b) 120 Phr
- 2- **Figure 2** (a) Dielectric constant and (b)  $\tan \delta$  for BF as a function of frequency at different temperatures
- 3- **Figure 3** (a) Dielectric constant and (b)  $\tan \delta$  for NR as a function of frequency at different temperatures
- 4- **Figure 4** Dependence of the dielectric constant on BF loading for (a) 293 K , (b) 353 K and (c) 393 K
- 5- **Figure 5** The variation of magnetic initial permeability with BF loading for RFC
- 6- **Figure 6** Loss tangent as function of BF content at different frequencies

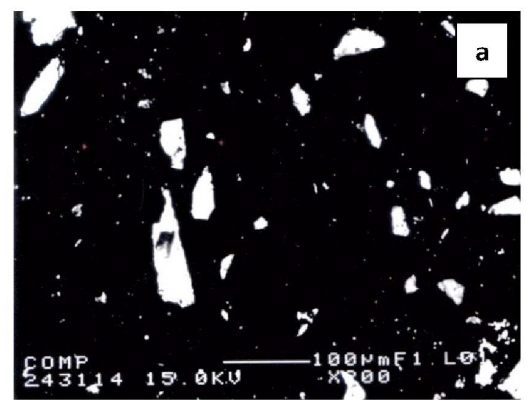


Fig. (1a)

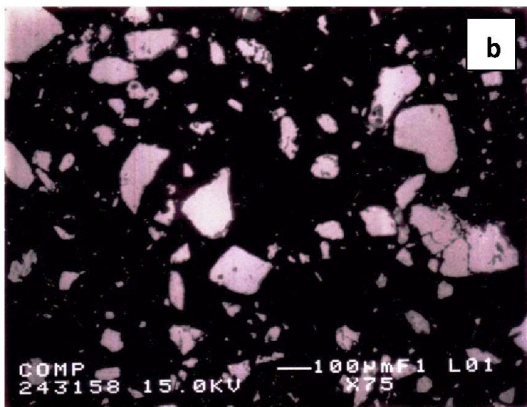


Fig. (1b)

**Figure 1** SEM images for the RFC , (a) 30 and (b) 120 Phr

Figure 1 SEM images for the RFC , (a) 30 and (b) 120 Phr

112x166mm (600 x 600 DPI)

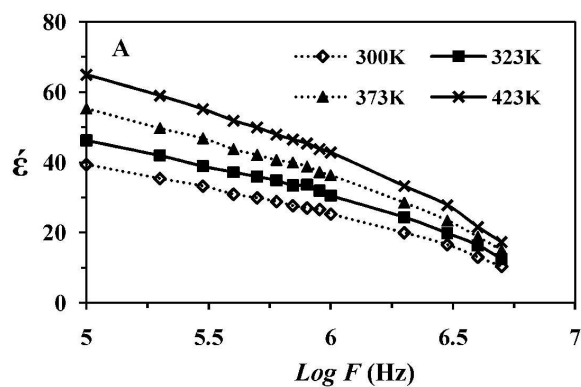


Fig. (2a)

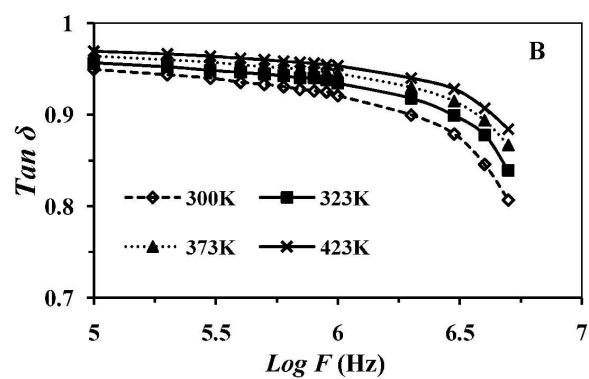


Fig. (2b)

**Figure 2** (a) Dielectric constant and (b)  $\tan \delta$  for BF as a function of frequency at different temperatures

Figure 2 (a) Dielectric constant and (b)  $\tan \delta$  for BF as a function of frequency at different temperatures  
154x192mm (600 x 600 DPI)

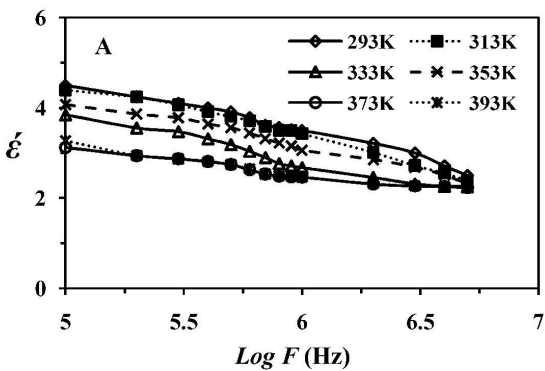


Fig.(3a)

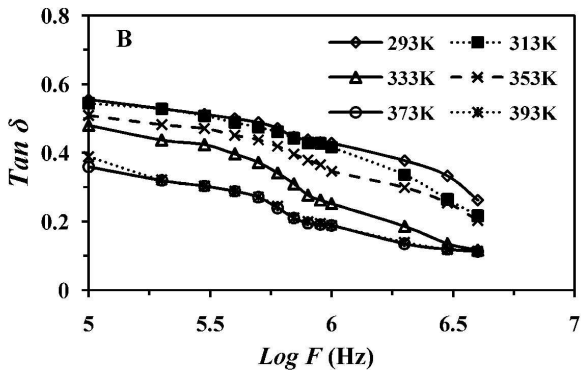


Fig. (3b)

**Figure 3** (a) Dielectric constant and (b)  $\tan \delta$  for NR as a function of frequency at different temperatures

Figure 3 (a) Dielectric constant and (b)  $\tan \delta$  for NR as a function of frequency at different temperatures  
166x184mm (600 x 600 DPI)

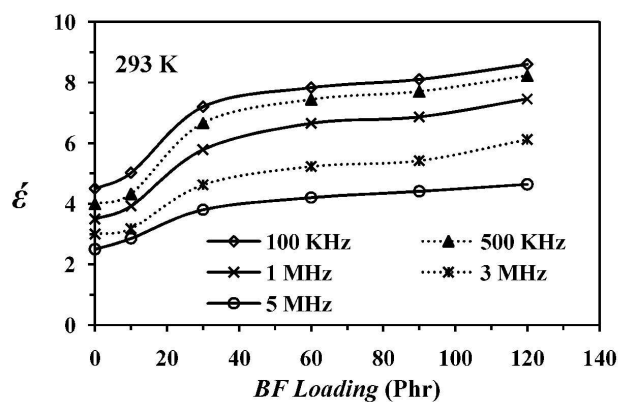


Fig. (4a)

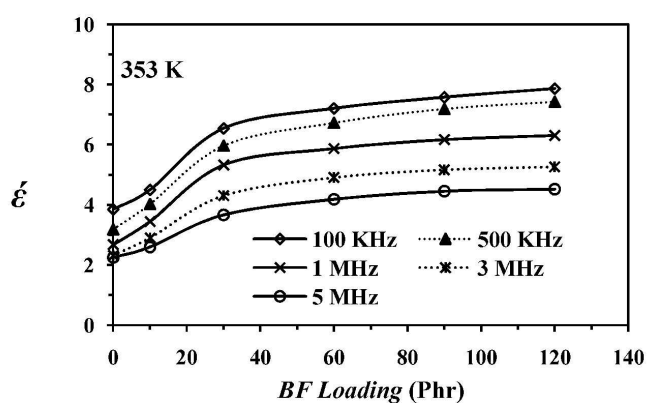


Fig. (4b)

**Figure 4** Dependence of the dielectric constant on BF loading for (a) 293 K, (b) 353 K and (c) 393 K

Figure 4 Dependence of the dielectric constant on BF loading for (a) 293 K, (b) 353 K and (c) 393 K  
166x174mm (600 x 600 DPI)

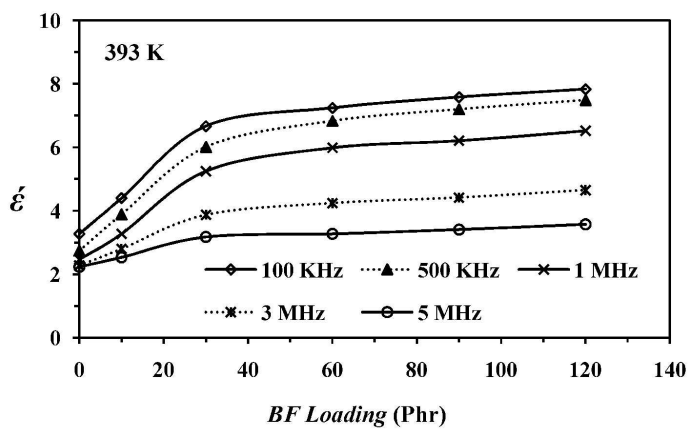


Fig. (4c)

**Figure 4** Dependence of the dielectric constant on BF loading for (a) 293 K , (b) 353 K and (c) 393 K

Figure 4 Dependence of the dielectric constant on BF loading for (a) 293 K , (b) 353 K and (c) 393 K  
173x157mm (600 x 600 DPI)



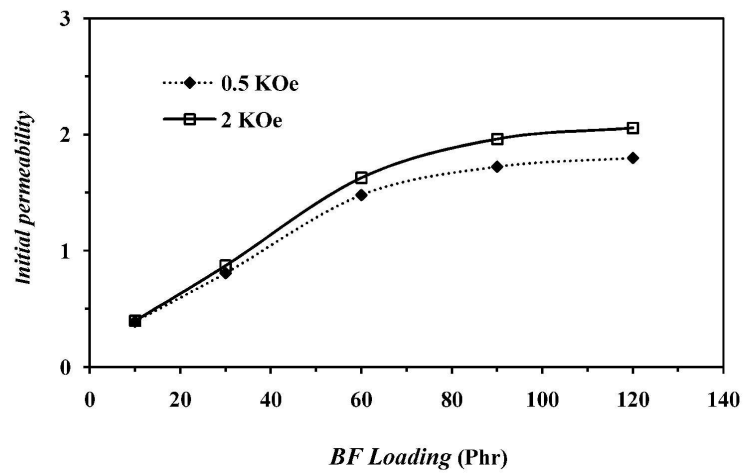


Fig.5

**Figure 5** The variation of magnetic initial permeability with BF loading for RFC

Figure 5 The variation of magnetic initial permeability with BF loading for RFC  
170x136mm (600 x 600 DPI)

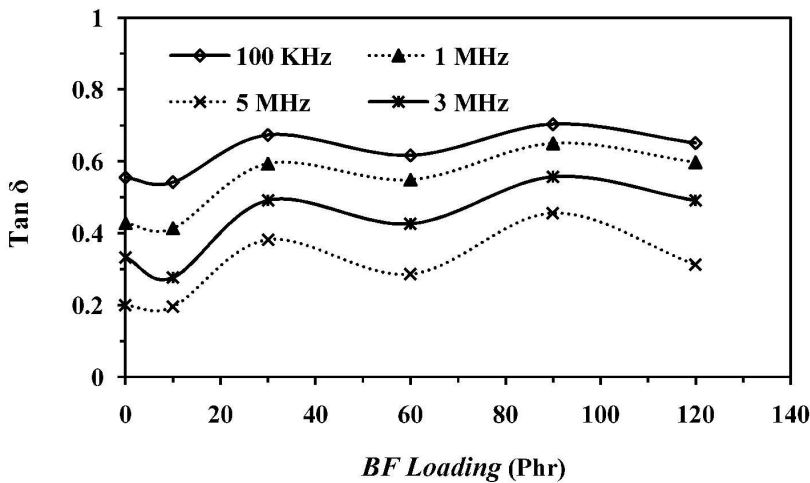


Fig. 6

**Figure 6** Loss tangent as function of BF content at different frequencies

Figure 6 Loss tangent as function of BF content at different frequencies  
148x121mm (600 x 600 DPI)